The Seasonal Cycle of Snow Cover, Sea Ice and Surface Albedo

ALAN ROBOCK

Department of Meteorology, University of Maryland, College Park 20742

(Manuscript received 14 August 1979, in final form 23 November 1979)

ABSTRACT

Satellite data are used to construct monthly mean snow cover maps for the Northern Hemisphere. The zonally averaged snow cover from these maps is calculated and used, along with zonally averaged sea ice cover and detailed data on land surface types, to calculate the seasonal cycle of zonally averaged surface albedo. A parameterization is presented of the solar zenith angle effect on ocean albedo. The effects of meltwater on the surface, solar zenith angle and cloudiness are all parameterized and included in the calculations of snow and ice albedo. It is found that meltwater effects are very important, but that zenith angle and cloudiness effects are negligible.

The albedo results for January, April, July, and October and the annual average results are compared to calculations by several other workers. The discrepancies are explained in terms of the above-mentioned effects and the averaging methods used. It is found that several other workers failed to weight the albedos by solar radiation when calculating annual averages. The global average surface albedo is calculated to be 0.150.

The data presented here allow a calculation of surface albedo for any land or ocean 10° latitude band as a function of surface temperature and ice and snow cover. The relationship between the seasonal cycles of snow and ice cover and surface temperature are also analyzed for possible use in a complete surface albedo parameterization for an energy balance climate model. The correct determination of the ice boundary is found to be more important than the snow boundary for accurately simulating the ice (and snow)-albedo feedback. Annual average calculations are also presented. Northern and Southern Hemisphere sea-ice-temperature regressions give differing results for the seasonal cycle but similar ones for annual average values.

1. Introduction

Surface albedo is one of the most important components of the climate system, and the changing snow and ice cover cause the largest changes in surface albedo. Not only do the snow and ice cover have a large seasonal cycle, but they also exhibit a substantial interannual variability. In addition the albedo of snow and ice exhibits a large seasonal cycle. In order to completely understand the climate system, these variations must be understood. As a first step in the process, this paper presents data on the mean zonally averaged seasonal surface albedo cycle. The data presented here include monthly average snow cover maps as well as zonal averages of snow cover, ice cover and surface albedo.

The next section presents maps derived from 10–12 years of satellite observations of the monthly average Northern Hemisphere (NH) snow cover for the seasonal cycle. While these data are zonally averaged for analysis in this paper, they also provide longitudinal information which may be used in other contexts. For example, general circulation models (GCM's) of the atmosphere commonly either employ fixed surface boundary conditions, including surface albedo, or calculate albedo as a function of surface wetness and/or snow cover from a hydrological model. The snow cover maps presented here are currently being used to specify surface albedo for the Goddard Laboratory for Atmospheric Sciences (GLAS) GCM, and for comparison with the calculated snow cover of the Geophysical Fluid Dynamics Laboratory (GFDL) GCM. The seasonal cycles of NH and Southern Hemisphere (SH) sea ice cover are then presented. Following this the surface albedos of various surface types are described. Particular attention is paid to the albedo of snow and ice and parameterizations of the effects of meltwater on the surface, solar zenith angle and cloudiness are presented. The next section describes the calculation procedure for zonally averaged surface albedo combining the observed distribution of surface types with the albedo observations and calculations.

The results of the calculations are presented next. They are compared with previous calculations by Sellers (1965), Schutz and Gates (1972a,b, 1973a, 1974a), Curran *et al.* (1979), Hummel and Reck (1979) and Kukla and Robinson (1979b). The present results are shown to be the most comprehensive, including the most accurate observations of snow and ice cover, the meltwater effect, detailed land surface type data, and weighting by solar radiation when calculating the annual average. The discrepancies

0027-0644/80/030267-19$08.75

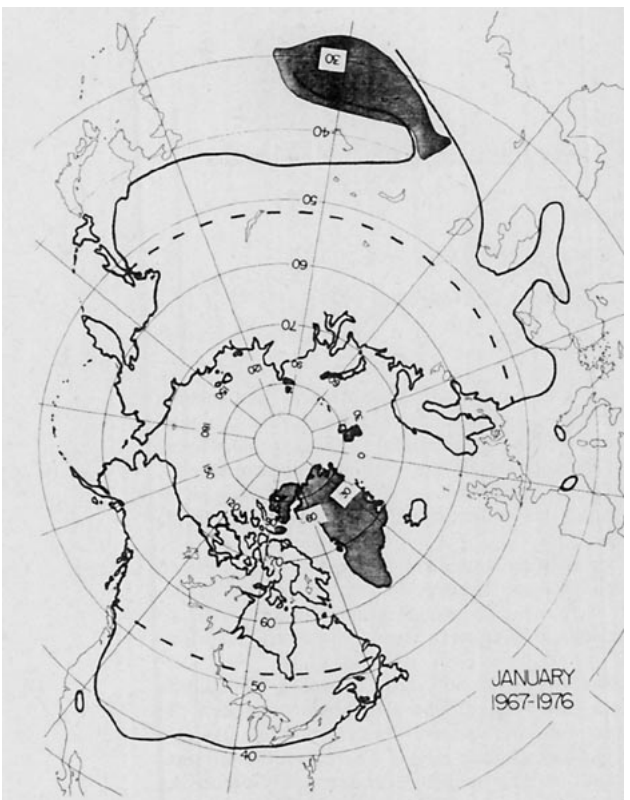

FIG. 1. Mean snow cover, January. The shaded areas in the Arctic are regions of permanent snow cover, and the shaded area at about 30°N, 90°E is the region of the Tibetan Plateau 4000 m in elevation. The shaded areas are not included in the zonal averages in Table 2. The data south of the dashed lines (52°N) for December, January, February and March come from Matson (1977). The data north of these lines and for the other months were constructed from unpublished monthly charts prepared by Matson at NESS. The dashed lines on other charts divide dark from light areas visible to the satellite.

between the various results are explained and are due mostly to these effects.

An accurate seasonal cycle of zonally averaged surface albedo is crucial to the calculation of the seasonal cycle of surface temperature in a seasonal energy balance climate model. The data presented here can be used to calculate the zonally averaged surface albedo for any land or ocean 10° latitude band for any month given the surface temperatures and the ice and snow fractional areas. Using the ice and snow data presented here, the mean seasonal cycle of temperature could be calculated without the feedback between ice and snow areas and temperature. If the ice and snow areas could be expressed as functions of surface temperature, then this formulation would constitute a complete surface albedo parameterization for use in an energy balance climate model. As a first step in developing such functions, the next section of this paper presents an analysis of the relationship between the observed cycles of snow and ice presented here and the observed cycles of land and ocean air temperatures. Annual average results are also presented.

The ice- (and snow-) albedo feedback (Schneider and Dickinson, 1974) is very important in determining the sensitivity of a climate model to forcing by climate change mechanisms. These include solar constant changes, carbon dioxide changes, stochastic forcing or any parameter change in the model. Until now, studies of this important feedback have been hampered by a poor knowledge of the variations of ice and snow. Of course when representing planetary albedo, atmospheric effects, particularly the zenith angle effect on clouds (Lian and Cess, 1977), must also be included correctly. Cloud albedo, though, has been shown to be a strong function of surface albedo (Kondrat'yev, 1965, pp. 390–391).

2. The seasonal cycle of snow

Monthly NH snow cover charts have been prepared by the National Environmental Satellite Service for each month since 1966 from satellite data. Previous studies using these data (Kukla and Kukla, 1974; Wiesnet and Matson, 1976) have described the technique and quality of the data, and Kukla and Robinson (1979a) have compared these data to other compilations and concluded that the data are sufficiently accurate for climate studies. These data were used in the present study to construct monthly mean show cover maps (Figs. 1–12).

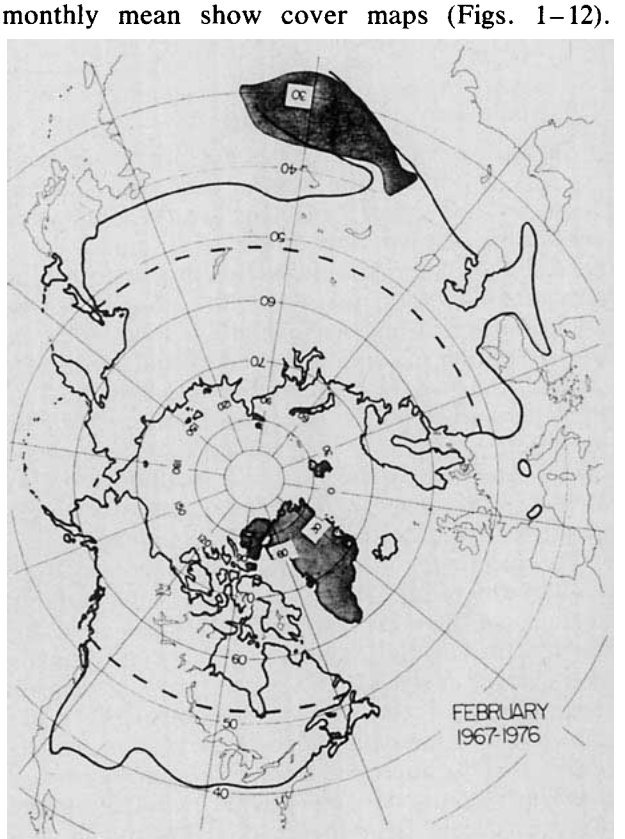

FIG. 2. As in Fig. 1 except for February.

FIG. 3. As in Fig. 1 except for March.

FIG. 4. As in Fig. 1 except for April.

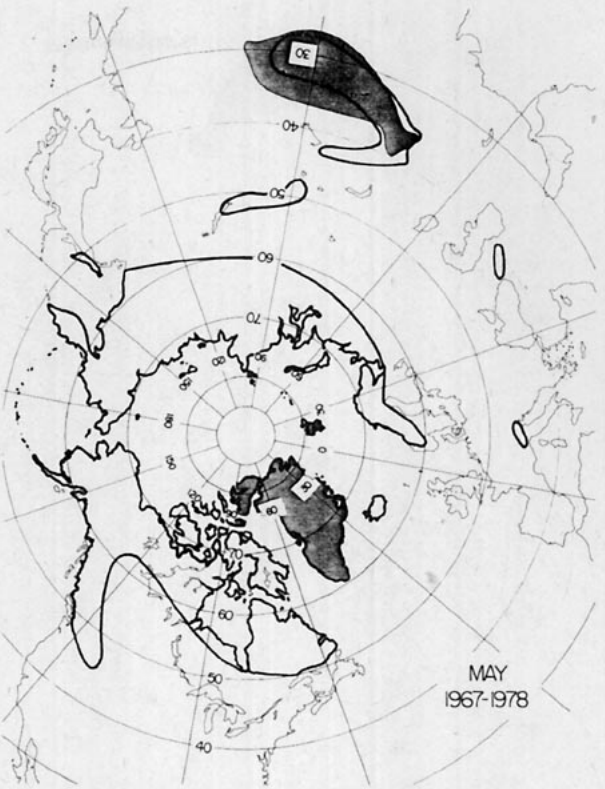

FIG. 5. As in Fig. 1 except for May.

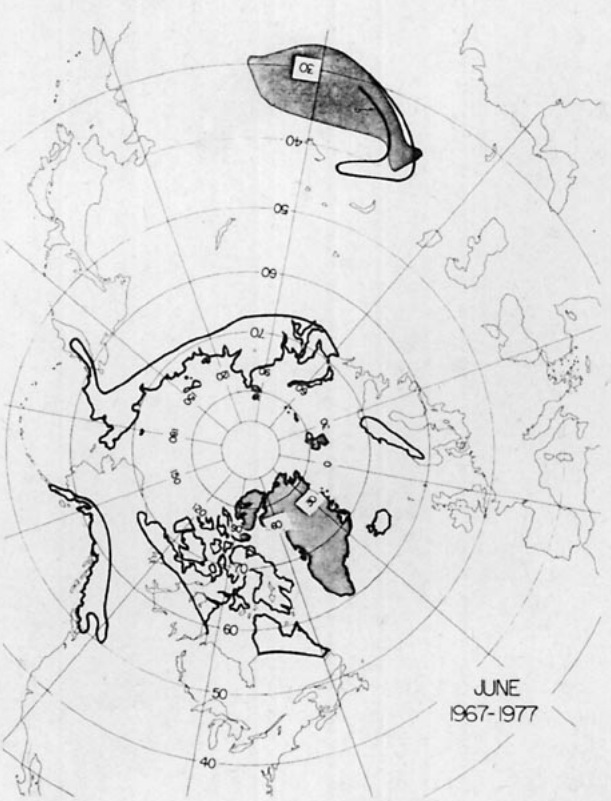

FIG. 6. As in Fig. 1 except for June.

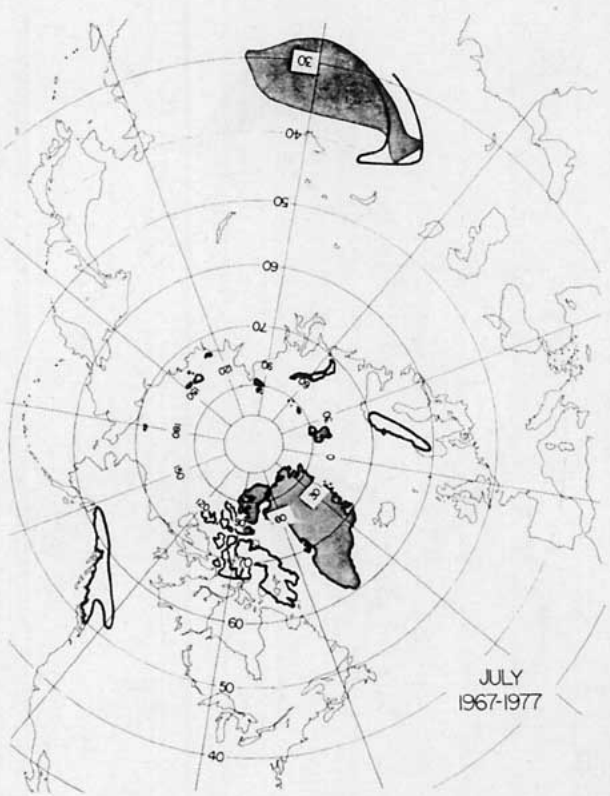

FIG. 7. As in Fig. 1 except for July.

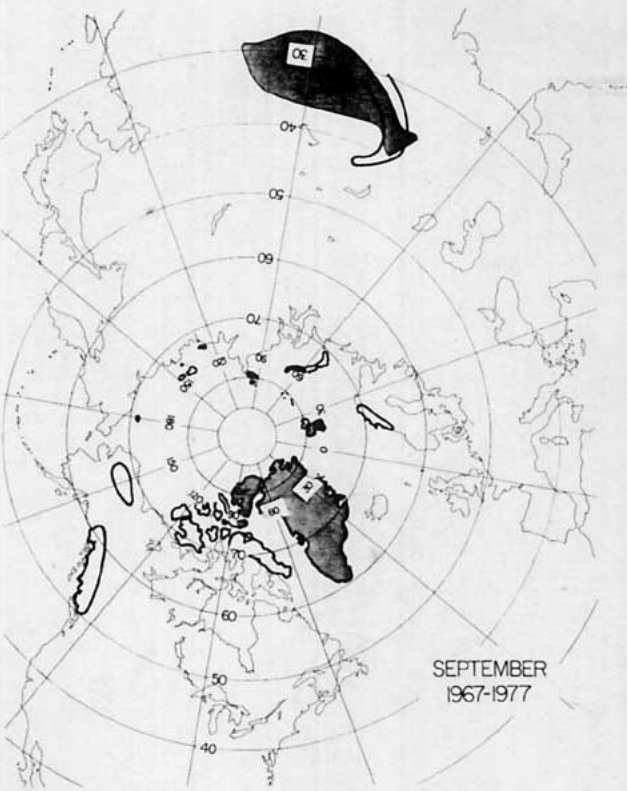

FIG. 9. As in Fig. 1 except for September.

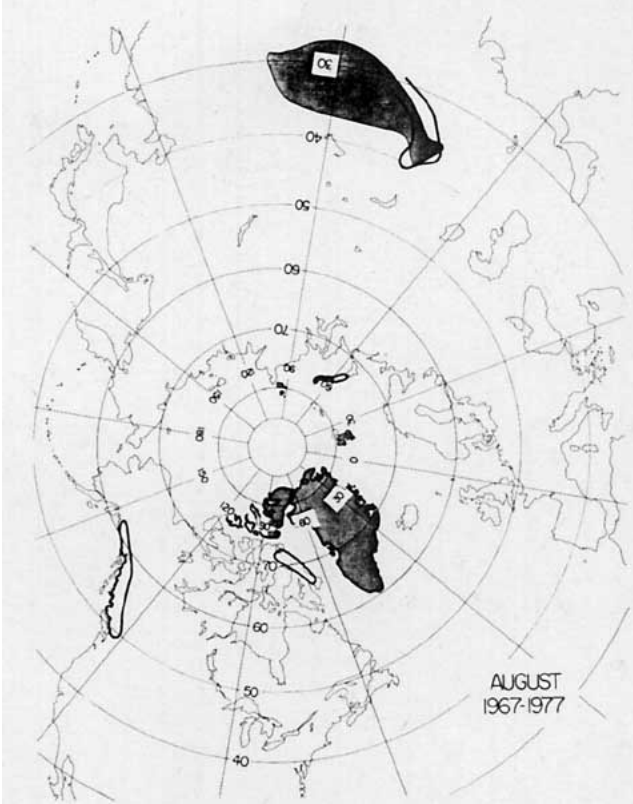

FIG. 8. As in Fig. 1 except for August.

FIG. 10. As in Fig. 1 except for October.

Matson (1977) has already constructed these maps for the months of December, January, February and March for the region south of 52°N. (The maps were originally requested for Skylab, whose orbit did not extend any further north.) His maps were used for these months with extensions north of 52°N taken from the original data. The maps for the other eight months were constructed using the same technique as Matson—by overlaying monthly maps for all the years of data on a light table and tracing the mean snow line. The errors involved in this technique are discussed in detail by Wiesnet and Matson (1976) and result from the subjective interpretations of a number of observers, combining a variety of satellites and sensors, the changing (increasing) skill of the meteorologists analyzing the weekly maps, and the subjectiveness of the analog averaging of weekly maps to monthly maps and individual monthly maps to ten-year average monthly maps. Although the maps do not all cover the same years, it is felt that the error thus introduced is no larger than the other errors discussed above. As Wiesnet and Matson point out, it is very hard to give a numerical value to the total error introduced at all stages of the procedure. Still, this data set is much more accurate and comprehensive than any previous study using ground-based observations (e.g., Hummel and Reck, 1979).

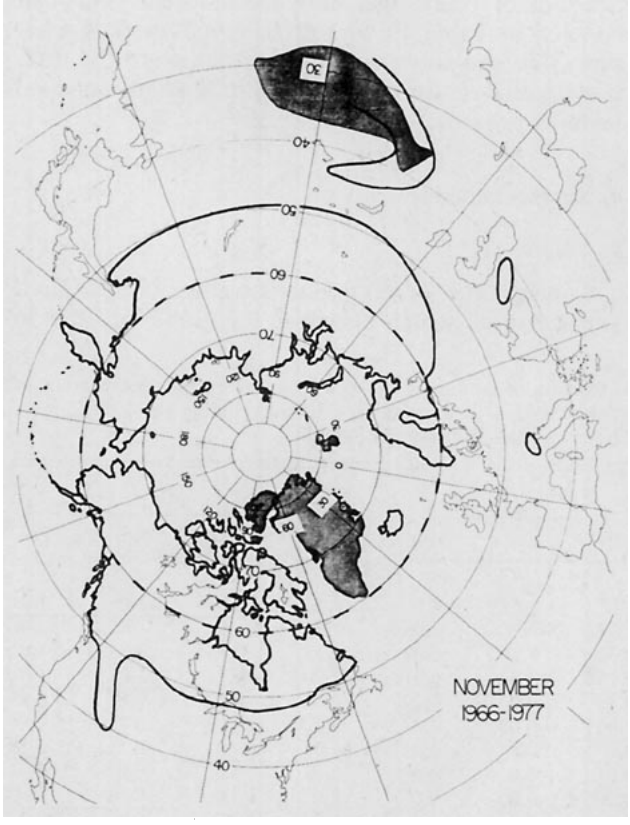

FIG. 11. As in Fig. 1 except for November.

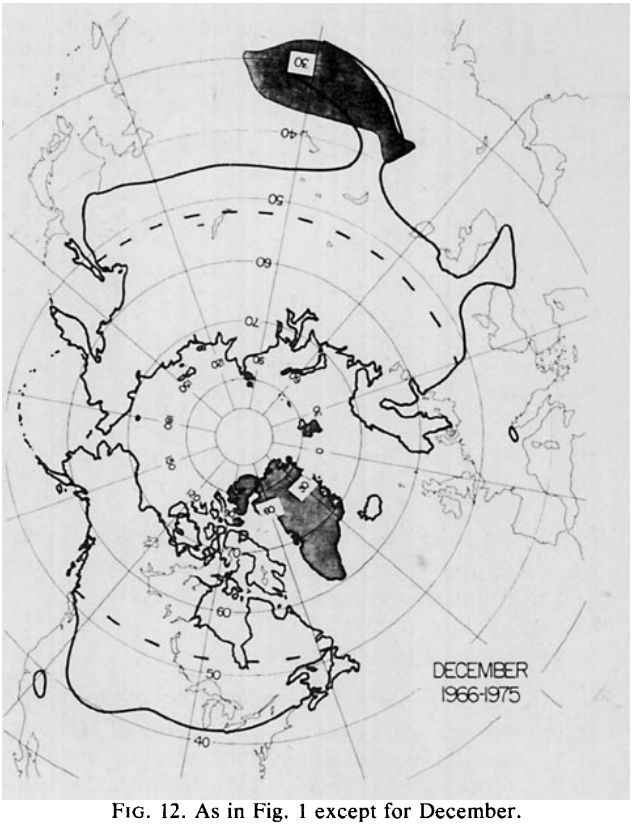

FIG. 12. As in Fig. 1 except for December.

A quantitative description of the seasonal cycle of the fractional snow cover as a function of latitude is presented in Table 1 for 5° latitude bands for the total ice and snow cover on *land*. For the purpose of studying the relationship between the zonal average snow cover and the zonal average surface temperature, however, I desired a snow cover data set for only those regions where surface temperature is thought to determine the snow cover. This would exclude regions with permanent ice caps which appear as snow in the satellite data. These regions are Greenland, Ellesmere Island, the eastern half of Devon Island, Axel Heiberg Island, Spitzbergen, the northern half of Novaya Zemlya and Severnaya Zemlya (Cohen, 1973; *Hammond Contemporary World Atlas*, 1972) and are marked with shading on the snow cover maps. In addition, the Tibetan plateau and Himalayan Mountains were thought to be regions where the snow cover was not related to the zonal average temperature at this latitude due to the extreme altitude and regions of permanent snow cover. This area above 4000 m altitude is also marked on the snow cover maps with shading. A new seasonal snow cover data set was calculated excluding the above areas (Table 2), and represents the fraction of the ice-free region (without Greenland, the Arctic Islands and Tibet) covered by snow. This data set, and not the total one shown

TABLE 1. Northern Hemisphere zonal average seasonal cycle of fraction of land area covered by snow. These data include land with permanent snow cover and come from Figs. 1–12 including the shaded areas. Latitudes for this and the next three tables indicate 5° latitude belts centered on them.

Latitude (°N)	Month											
	Jan	Feb	Mar	Apr	May	Jun	Jul	Aug	Sep	Oct	Nov	Dec
82.5	1.0	1.0	1.0	1.0	1.0	1.0	1.0	1.0	1.0	1.0	1.0	1.0
77.5	1.0	1.0	1.0	1.0	1.0	1.0	0.86	0.86	0.86	1.0	1.0	1.0
72.5	1.0	1.0	1.0	1.0	0.99	0.98	0.46	0.32	0.51	1.0	1.0	1.0
67.5	1.0	1.0	1.0	1.0	0.98	0.55	0.17	0.10	0.22	0.99	1.0	1.0
62.5	1.0	1.0	1.0	1.0	0.76	0.17	0.07	0.04	0.03	0.77	1.0	1.0
57.5	0.97	0.97	0.95	0.84	0.32	0.14	0.04	0.02	0.02	0.30	0.88	0.93
52.5	0.91	0.91	0.79	0.55	0.22	0.04	0.02	0.02	0.02	0.08	0.71	0.86
47.5	0.87	0.86	0.70	0.17	0.06	0.00	0.00	0.00	0.01	0.01	0.11	0.78
42.5	0.67	0.70	0.20	0.08	0.04	0.03	0.00	0.00	0.01	0.03	0.10	0.33
37.5	0.20	0.23	0.15	0.07	0.05	0.04	0.04	0.03	0.02	0.07	0.08	0.14
32.5	0.15	0.17	0.17	0.16	0.10	0.05	0.10	0.10	0.11	0.13	0.14	0.14

in Table 1, was used to derive the regression equations relating snow cover to surface temperature and to calculate the seasonal albedo cycle.

3. The seasonal cycle of sea ice

Table 3 presents the mean seasonal cycle of NH fractional sea ice cover as a function of latitude. It is essentially the same data set compiled by Walsh (1978) for the years 1953–77, with the addition of "Sea Ice Normals" data for 1966–74 from the British Meteorological Office (1977) for ice in the Sea of Okhotsk and Baltic Sea which were omitted by Walsh because of incomplete data. Walsh (1978) and Walsh and Johnson (1979) discuss the quality of the data and present detailed analysis of the ice area fluctuations. Note that the fractional ice areas presented in Table 3 are centered on the *end* of each month, not the middle of the month as was done for Tables 1, 2 and 4.

Table 4 presents the zonally averaged SH fractional sea ice cover. The data come from Curran *et al.* (1979, Table 4) and were obtained from the ESMR instrument on Nimbus 5 from July 1973 to October 1974. This SH sea ice data set is of poorer quality than the NH data both because of its limited time period, which may or may not have been representative, and because of ambiguities in transforming microwave brightness temperatures into sea ice concentrations. Since SH snow cover data are not readily available, NH data offset by six months because of the difference in the seasons were used in the albedo calculations. The errors involved in this are very small due to the small area of the SH subject to seasonal snow fluctuations. (This can be seen in Table 10 where the zonal average fractional ice and snow cover is very close to the fractional ice cover for latitudes 30–70°S where seasonal snow is present.)

4. Surface albedos

a. Surface type

Cohen (1973, p. 99) presents a global map of land surface type, which classifies the globe into the 16

TABLE 2. Northern Hemisphere zonal average seasonal cycle of fraction of land area covered by snow excluding the areas of permanent snow cover and the Tibetan Plateau over 4000 m in elevation. The data come from Figs. 1–12 excluding the shaded areas. The boxed data in this and the next two tables were not used in the regressions discussed in Section 7.

Latitude (°N)	Month											
	Jan	Feb	Mar	Apr	May	Jun	Jul	Aug	Sep	Oct	Nov	Dec
82.5												
77.5	1.0	1.0	1.0	1.0	1.0	1.0	0.5	0.5	0.5	1.0	1.0	1.0
72.5	1.0	1.0	1.0	1.0	0.99	0.98	0.26	0.08	0.34	1.0	1.0	1.0
67.5	1.0	1.0	1.0	1.0	0.98	0.52	0.10	0.02	0.15	0.99	1.0	1.0
62.5	1.0	1.0	1.0	1.0	0.76	0.15	0.04	0.01	0.00	0.77	1.0	1.0
57.5	0.97	0.97	0.95	0.84	0.32	0.14	0.04	0.02	0.02	0.30	0.88	0.93
52.5	0.91	0.91	0.79	0.55	0.22	0.04	0.02	0.02	0.02	0.08	0.71	0.86
47.5	0.87	0.86	0.70	0.17	0.06	0.0	0.0	0.0	0.01	0.01	0.11	0.78
42.5	0.46	0.49	0.17	0.06	0.01	0.0	0.0	0.0	0.0	0.0	0.07	0.31
37.5	0.13	0.14	0.07	0.01	0.0	0.0	0.0	0.0	0.0	0.0	0.01	0.08
32.5	0.01	0.02	0.02	0.02	0.0	0.0	0.0	0.0	0.0	0.0	0.0	0.0

TABLE 3. Northern Hemisphere zonal average seasonal cycle of fraction of ocean area covered by sea ice. The data were provided by John Walsh and were supplemented by data from the British Meteorological Office (1977). They are averages for the period 1953–77, and are for the *end* of each month, rather than the monthly average as in Tables 1, 2 and 4.

Latitude (°N)	Month											
	Jan	Feb	Mar	Apr	May	Jun	Jul	Aug	Sep	Oct	Nov	Dec
87.5	1.0	1.0	1.0	1.0	1.0	1.0	1.0	1.0	1.0	1.0	1.0	1.0
82.5	1.00	1.0	1.00	1.00	1.00	0.99	0.98	0.96	0.98	1.00	1.00	1.00
77.5	0.93	0.93	0.93	0.93	0.91	0.83	0.73	0.62	0.65	0.81	0.88	0.91
72.5	0.76	0.77	0.77	0.76	0.73	0.63	0.47	0.31	0.32	0.61	0.71	0.74
67.5	0.57	0.59	0.59	0.56	0.48	0.36	0.21	0.07	0.06	0.26	0.45	0.53
62.5	0.43	0.46	0.46	0.38	0.24	0.14	0.03	0.01	0.00	0.02	0.20	0.36
57.5	0.25	0.28	0.28	0.19	0.11	0.07	0.01	0.00	0.00	0.00	0.03	0.17

surface types shown in Table 5. The fractions of each type were digitized to 10° latitude bands. Ice caps were assumed to occupy the shaded regions (Figs. 1–12) in the Arctic, half of the shaded Himalayan region, and all of Antarctica. Because of the treatment of snow and ice (Sections 4d and 5) the surface types were combined into six surface categories as shown in Table 6. Table 7 presents the fraction of each of these categories by latitude band.

b. Snow-free land albedos

Albedos of the various land surface types are listed in Table 5 with references. Hummel and Reck (1979), who present a static surface albedo calculation for four seasons, distinguished between the albedo of deciduous and coniferous forests. I feel, however, from looking at the references in Table 5, that the large variety of overlapping measurements for both types of forest do not justify this distinction.

The albedos of the various land surface types are all very close, except for sand deserts, when compared to snow albedos, discussed later. This contrast is what produces the snow-albedo feedback. Several other factors which may affect the seasonal land albedo cycle, such as the spectral dependence of albedo, soil moisture, biological changes, farming and solar zenith angle dependence were not considered, because the changes produced would be much smaller than that caused by snow. (Solar zenith angle corrections are applied to ocean, snow and ice albedos as discussed later.) The albedo values that are used, however, are integrated over the spectrum, and integrated over the diurnal cycle. Soil moisture consideration would require assumptions about precipitation. In addition, the other effects are poorly known. In the future, a more detailed surface albedo calculation should include them. When considering ice age time scales, changes in the surface types may also be important (Williams *et al.*, 1974; CLIMAP Project Members, 1976; Cess, 1978).

c. Water albedo

It was determined from the observations of Payne (1972) that sea surface albedos (α_s) for different months and latitudes fit the formula

$$\alpha_s = 0.06/\cos\gamma, \quad (1)$$

where γ = (latitude − solar declination)/1.2. These values, which depend only on solar zenith angle for their time dependence, were used for each month and latitude, for ocean and inland water surfaces.

d. Snow and ice albedos

The albedo of snow depends not only on the underlying surface type, but also on the temperature, age of the snow, cloudiness and solar zenith

TABLE 4. Southern Hemisphere zonal average seasonal cycle of fraction of ocean area covered by sea ice. Data are from Curran *et al.* (1979, Table 4).

Latitude (°S)	Month											
	Jan	Feb	Mar	Apr	May	Jun	Jul	Aug	Sep	Oct	Nov	Dec
77.5	0.96	0.95	1.00	1.00	1.00	1.00	1.00	1.00	1.00	1.00	1.00	1.00
72.5	0.90	0.82	0.88	0.99	1.00	1.00	1.00	1.00	1.00	1.00	1.00	0.99
67.5	0.47	0.26	0.32	0.60	0.77	0.87	0.93	0.95	0.95	0.94	0.90	0.71
62.5	0.05	0.01	0.03	0.11	0.29	0.48	0.63	0.69	0.70	0.70	0.52	0.23
57.5	0.0	0.0	0.0	0.0	0.01	0.04	0.10	0.19	0.23	0.22	0.13	0.04

TABLE 5. Albedos of different surface types. References for snow-free albedos are indicated by letters where H is Hummel and Reck (1979), P is Posey and Clapp (1964), M is Miranova (1973) and K is Kung *et al.* (1964). References for snow and snow with meltwater are discussed in the text.

Surface type	Snow-free	(Reference)	Snow	Meltwater
1. Ice cap	Same as snow		0.80	0.40
2. Tundra	0.17	(H)	0.80	0.40
3. Inland water	Same as ocean		0.75 (ice)	0.40
4. Deciduous forest	0.15	(H, P / M, K)	0.40	0.30
5. Mixed deciduous & coniferous forest	0.15		0.40	0.30
6. Coniferous forest	0.15		0.40	0.30
7. Equatorial forest	0.07	(H, P)	—	—
8. Arable & mixed farming	0.15	(H, M, K)	0.80	0.40
9. Rice paddy	0.12	(H)	—	—
10. Other irrigated land	0.20	(H, K)	0.80	0.40
11. Grazing	0.18	(H, K, M)	0.80	0.40
12. Tropical woodland & grassland	0.16	(H)	—	—
13. Marsh or Bog	0.14	(K, M)	0.80	0.40
14. Sand desert	0.42	(H)	—	—
15. Shrubland desert	0.22	(H, P, K)	0.80	0.40
16. Ocean	Eq. (1)		0.75 (ice)	0.40

angle. Ice albedo behaves the same way. In order to accurately express snow albedo, the land surface was divided into several categories (Table 6); unforested land on which snow falls, forests with seasonal snow, ice caps with permanent snow, and land on which snow never falls (equatorial surface types and sand desert).

The temperature dependence of snow and ice is such that higher temperatures cause a lower albedo due to meltwater pockets on the surface and changes in the crystal structure. In addition, on a daily basis, debris accumulates on the surface during the melting season, lowering the albedo (Petzold, 1977), but this effect was not thought to be important for 15- or 30-day averages. The snow and ice albedo were assumed to vary linearly from a "snow" value for $T \leq -10°C$ to a "meltwater" value for $T \geq 0°C$ (Petzold, 1977; Doronin, 1970). The snow value for flat surfaces was chosen to be 0.80 and the meltwater value to be 0.40 (Kondrat'yev, 1965, Miranova, 1973; Doronin, 1970; Rusin, 1964, Chernigovskii, 1963). For forests, the corresponding values are 0.40 and 0.30 (Kondrat'yev, 1965; Posey and Clapp, 1964; Hummel and Reck, 1979; Miranova, 1973; Kung *et al.*, 1974). For sea ice, including the effects of snow on the ice and breaks in the ice, the values are 0.75 and 0.40 (Miranova, 1973; Vowinckel and Orvig, 1970). This effect is in addition to the changes in snow and ice area as temperature changes. Thus as temperature rises, snow and ice area and albedo both decrease.

Rusin (1964) and Petzold (1977) both point out the effects of clouds on snow albedo, with high cloudiness producing more diffuse radiation which has a higher albedo. As the above values are for average cloudiness, this effect was included by increasing the snow or ice albedo by 5% with clouds and decreasing it by 5% for clear areas. The climatological seasonal and latitudinal fractional cloud distribution was determined from London (1957) for the NH, Sasamori *et al.* (1972) for the SH and Vowinckel and Orvig (1970) for high NH latitudes.

At high solar zenith angles, the albedo of snow and ice increases and has been measured by Petzold (1977). This correction was applied by adding a percentage of the albedo (δ) to the albedo (Petzold, personal communication):

$$\delta = 0.01766 \sec Z - 0.0221, \quad 0\% \leq \delta \leq 50\%, \quad (2)$$

where Z is the noon solar zenith angle.

TABLE 6. Categories of surface types used to calculate areal average albedos.

Surface category	Includes these surface types (see Table 5)
a. Ocean	16
b. Inland water	3
c. Unforested land, seasonal snow	2, 8, 10, 11, 13, 15
d. Forest, seasonal snow	4, 5, 6
e. Ice cap	1
f. Land, no snow ever	7, 9, 12, 14

5. Albedo calculations

This section describes the calculation procedure to give the zonally averaged surface albedo for any 10° latitude band at any time. The snow and ice fractional areas come from Tables 2–4. As accurate parameterizations are developed, they could be calculated as a function of surface temperature. Ice areas for inland water (F_{ii}) were assumed to be the same as ocean values. If they are to be calculated

TABLE 7. Fraction of 10° latitude bands covered by various surface categories (see Table 6), area weighted means of fraction times albedo for three of the categories (c, d and f) and S parameter, explained in text and calculated in (3). The fractional areas were calculated from data provided by John Hummel who digitized data from Cohen (1973, p. 99).

Latitude	F_a	F_b	F_c	F_d	F_e	F_f	$F_c\alpha_c$	$F_d\alpha_d$	$F_f\alpha_f$	S
85°N	0.9030	0.0	0.0448	0.0	0.0522	0.0	0.0076	0.0	0.0	1.000
75°N	0.6960	0.0	0.1999	0.0	0.1041	0.0	0.0340	0.0	0.0	1.000
65°N	0.2950	0.0333	0.3120	0.3202	0.0394	0.0	0.0527	0.0480	0.0	1.000
55°N	0.4230	0.0020	0.3339	0.2404	0.0	0.0007	0.0547	0.0361	0.0003	1.001
45°N	0.4770	0.0303	0.3735	0.0914	0.0032	0.0246	0.0652	0.0137	0.0103	1.049
35°N	0.5720	0.0025	0.3289	0.0290	0.0300	0.0376	0.0590	0.0043	0.0108	1.096
25°N	0.6240	0.0	0.2540	0.0188	0.0	0.1032	0.0497	0.0028	0.0265	1.378
15°N	0.7370	0.0	0.1410	0.0042	0.0	0.1179	0.0257	0.0006	0.0163	1.812
5°N	0.7720	0.0006	0.0634	0.0	0.0	0.1640	0.0109	0.0	0.0194	3.563
5°S	0.7640	0.0009	0.0577	0.0217	0.0	0.1556	0.0095	0.0033	0.0122	2.936
15°S	0.7800	0.0	0.1079	0.0541	0.0	0.0581	0.0188	0.0081	0.0072	1.359
25°S	0.7680	0.0	0.2010	0.0040	0.0	0.0270	0.0366	0.0006	0.0093	1.132
35°S	0.8860	0.0	0.1046	0.0089	0.0	0.0005	0.0184	0.0013	0.0002	1.004
45°S	0.9690	0.0	0.0215	0.0095	0.0	0.0	0.0040	0.0014	0.0	1.000
55°S	0.9910	0.0	0.0005	0.0004	0.0080	0.0	0.0001	0.0001	0.0	1.000
65°S	0.9050	0.0	0.0	0.0	0.0950	0.0	0.0	0.0	0.0	1.000
75°S	0.2690	0.0	0.0	0.0	0.7310	0.0	0.0	0.0	0.0	1.000
85°S	0.0	0.0	0.0	0.0	1.0000	0.0	0.0	0.0	0.0	1.000

it is suggested that they be calculated using the ocean formula, but with land temperatures. The snow fractional areas must be restricted only to those surface types which receive snow and so are multiplied by a factor S

$$S = F_L/\sum (F_b + F_c + F_d + F_e), \qquad (3)$$

where F_L is the total fraction of land and F_{b-e} are given in Table 7. The snow and ice albedos are calculated as indicated in Section 4d with the appropriate corrections. The albedo for any latitude band is then

$$\begin{aligned}\alpha = {} & F_a(\alpha_s(1 - F_i) + \alpha_i F_i) \\ & + F_b(\alpha_s(1 - F_{ii}) + \alpha_{ii} F_{ii}) \\ & + F_c(\alpha_c(1 - F_s S) + \alpha_{sn} F_s S) \\ & + F_d(\alpha_d(1 - F_s S) + \alpha_{sf} F_s S) \\ & + F_e \alpha_{sn} \\ & + F_f \alpha_f, \end{aligned} \qquad (4)$$

where F_{a-f} is the fraction of surface category as given in Table 7, α_s the sea surface albedo (1), F_i

TABLE 8. Seasonal cycle and annual average of zonal average surface albedo (in percent) for 10° latitude bands calculated with (4).

Latitude	Jan	Feb	Mar	Apr	May	Jun	Jul	Aug	Sep	Oct	Nov	Dec	Annual average: Radiation weighted	Annual average: Unweighted
85°N	95.0	95.0	81.8	77.1	77.8	48.7	41.4	41.8	72.9	89.4	94.6	95.0	57.1	76.1
75°N	82.5	81.3	71.9	71.3	64.3	38.0	30.7	27.6	33.8	61.5	76.1	80.9	45.7	60.3
65°N	60.8	57.5	56.3	50.4	29.5	21.6	17.0	15.4	16.2	36.4	52.6	63.2	28.6	39.7
55°N	43.0	42.5	37.0	22.2	16.3	13.7	12.7	12.5	12.9	15.6	32.8	42.6	19.5	25.2
45°N	31.6	27.1	17.8	13.8	12.7	12.3	12.3	12.4	12.8	13.4	15.0	25.3	15.1	17.1
35°N	14.3	13.8	13.0	12.4	12.2	12.1	12.1	12.2	12.5	12.9	13.5	14.2	12.7	12.9
25°N	12.7	12.3	12.0	11.8	11.7	11.7	11.7	11.7	11.9	12.2	12.5	12.8	12.0	12.1
15°N	9.4	9.1	8.8	8.7	8.7	8.7	8.7	8.7	8.8	9.0	9.3	9.5	8.9	8.9
5°N	8.0	7.8	7.7	7.7	7.8	7.8	7.8	7.7	7.7	7.8	7.9	8.1	7.8	7.8
5°S	7.2	7.1	7.1	7.2	7.4	7.5	7.4	7.3	7.1	7.1	7.2	7.3	7.2	7.2
15°S	8.1	8.1	8.2	8.4	8.7	8.9	8.8	8.5	8.2	8.1	8.1	8.1	8.3	8.4
25°S	9.3	9.3	9.5	9.9	10.4	10.7	10.5	10.1	9.7	9.4	9.3	9.2	9.7	9.8
35°S	7.4	7.6	8.0	8.7	9.5	10.1	9.9	9.2	8.3	7.7	7.4	7.4	8.1	8.4
45°S	6.7	7.0	7.7	8.8	10.3	11.5	11.1	9.8	8.3	7.3	6.8	6.6	7.7	8.5
55°S	7.0	7.5	8.6	10.4	12.9	14.9	15.0	14.2	12.9	11.5	9.4	7.6	9.4	11.0
65°S	20.2	18.4	23.5	35.7	50.8	67.3	69.4	68.1	67.2	61.9	45.8	28.3	35.7	46.4
75°S	74.6	77.6	79.4	83.9	94.1	94.2	94.3	94.2	81.0	79.9	79.6	74.6	77.2	83.9
85°S	80.7	81.1	83.6	95.0	95.0	95.0	95.0	95.0	89.2	81.5	80.6	80.5	80.9	87.8

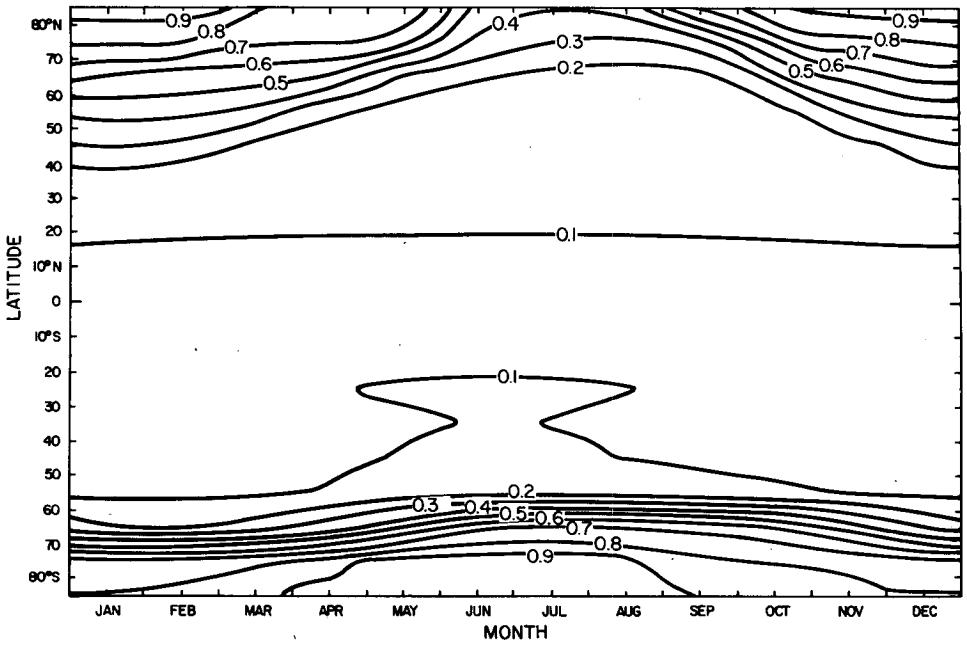

FIG. 13. The seasonal cycle of surface albedo calculated using (4). This corresponds to the data in Table 8.

the fractional ice area, α_i the ice albedo, F_{ii} the inland ice area, α_{ii} the inland ice albedo using land temperature, α_c the surface type-weighted average albedo for category c, F_s the fractional snow area, α_{sn} the snow albedo for flat land, S the snow factor (3), α_d the weighted albedo for category d, α_{sf} the snow albedo for forests and α_f the weighted albedo for category f. $F_c\alpha_c$, $F_d\alpha_d$ and $F_f\alpha_f$ are constants and are given in Table 7 along with S. The snow is implicitly assumed to have the same fractional area for surface categories c and d with this formulation. Implicit in the calculation of albedo using (4) are the meltwater, cloud and zenith angle corrections to the ice and snow albedos: α_i, α_{ii}, α_{sn} and α_{sf}. The albedo is required to be less than or equal 0.95, but this value is only reached in the polar winters where it is of no consequence.

In order to calculate snow and ice albedo as a function of temperature, the seasonal cycle of surface air temperature over land (T_L) and over the sea (T_s) was obtained as follows. The seasonal cycle of zonally averaged surface air temperature (T_z) was obtained from Crutcher and Meserve (1970) and Taljaard *et al.* (1969) at 5° intervals in latitude (90°N, 85°N, . . .). The difference between land and water air temperatures was obtained from Schutz and Gates (1971, 1972a,b, 1973a,b, 1974a,b) for January, April, July and October. The differences were linearly interpolated between these months for the other eight months. The differences and zonal averages were then linearly interpolated in latitude to give temperatures centered on 5° latitude bands (87.5°N, 82.5°N, . . .). Finally, the differences and zonal averages were combined algebraically with fractional land and sea amounts for each latitude band to give land and sea temperatures.

6. Discussion of calculated albedo

In this section the seasonal cycle of zonally averaged surface albedo calculated according to the previous section is presented and compared to previous results. The effects of several assumptions in the albedo calculation are discussed and the desirability of using radiation weighted albedo is emphasized.

The calculated albedos are shown in Table 8 and Fig. 13. (The table only gives mid-month values, but the calculations were done at half-month time steps and these results were used for the figure.) Near the North Pole a large seasonal cycle is seen due to the combined effects of the changing snow and ice areas and the changing snow and ice albedos. The minimum and maximum values are displaced somewhat from the solstices due to the thermal lags in the snow and ice areas and in the temperatures which influence the albedos. The large fraction of oceans at latitudes from 20°N to 60°S is reflected in a region with albedos below 0.1, except for the maximum from 20 to 60°S in the SH winter which is a zenith angle effect on the water albedo. The midlatitudes of the NH show a much larger seasonal cycle than the corresponding SH latitudes. This is due mainly to the seasonal snow cover cycle in the NH, which has a much higher percentage of land.

Fig. 14 presents the zonal average albedo for four months along with the annual average albedo. The

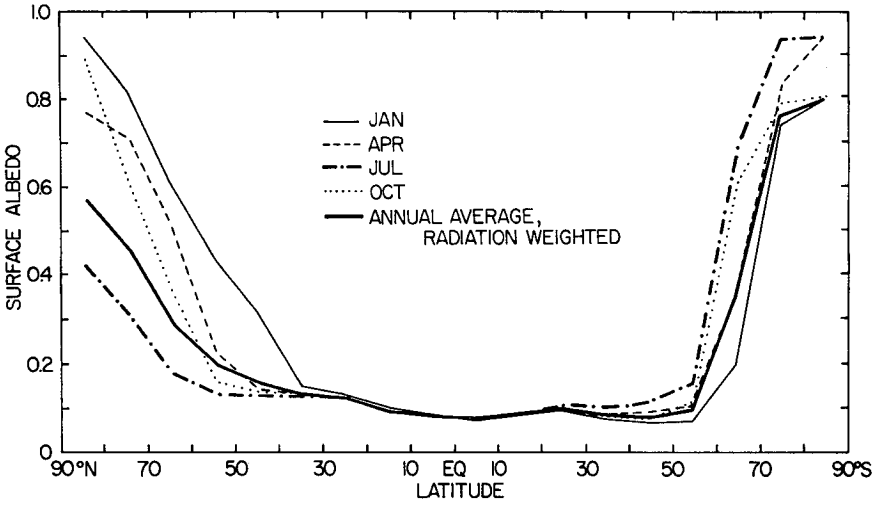

FIG. 14. The annual average surface albedo, radiation weighted, plotted with values from four months. Data are from Table 8.

annual average was calculated by weighting the individual month's albedo by the amount of incoming solar radiation at the top of the atmosphere for that month and latitude, i.e.,

$$\bar{\alpha}(\phi) = \frac{\sum \alpha(\phi) S(\phi)}{\sum S(\phi)}, \qquad (5)$$

where $\alpha(\phi)$ is the albedo for a given latitude band, $S(\phi)$ the incoming solar radiation, the bar represents an annual average and the summation is over all the months. (A more exact way to do the weighting would be by solar radiation at the bottom of the atmosphere, including the effects on atmospheric transmissivity of cloudiness, solar zenith angle and atmospheric composition. The appropriate corrections are not well understood and would introduce only minor changes to results calculated here.) When using albedo data to study radiation climatology it is very important that the averaging be done this way. Otherwise, high values at the winter poles will be included in the average even though they have no effect on the radiation. Annual average climate models should use albedos which are the same as this radiation weighted annual average and not an unweighted average. It is easily seen from Fig. 14 how the average is weighted toward the summer values in each hemisphere. The seasonal range is also illustrated by the cover for the four representative months. The difference between radiation weighted and unweighted annual averages is also illustrated in Table 8 and Fig. 19, which also includes the results of other calculations of surface albedo. The unweighted albedo is much higher at the poles, but it is not representative of annual average ability of the surface to reflect radiation.

Figs. 15–18 give the albedo values calculated with (4) for January, April, July and October and compare them to three other calculations. The reasons for the differences between my calculations and the others are discussed later in the context of annual average values, but the major discrepancies in the monthly values are pointed out here. My high polar winter values are due to the zenith angle correction, but are not of consequence when radiation weighted. The high values of Curran *et al.* (1979) for January, April and October in the NH midlatitudes are due to the high albedos chosen for snow (0.75) and land (0.18). Curran *et al.* (1979) and Kukla and Robinson (1979b) obtained high NH polar values in July because they did not include the meltwater effects on snow and ice albedo. The high albedo values at 62 and 66°S from Schutz and Gates (1973a) for April are probably an error as the Posey and Clapp (1964) map for April, from which the Schutz and Gates data were derived, indicates a much lower albedo.

Fig. 19 includes annual average surface albedo results from five other sources. Sellers (1965, Table 1) used data obtained in the 1950's and the results were radiation weighted (personal communication). His results are very similar to mine except in the NH midlatitudes and SH high latitudes. It is possible that since his data were taken during a time when the NH was substantially warmer, that there was less snow then. Perhaps a more likely explanation is that without satellite data, his knowledge of the snow and ice extent was not as good, and this could also explain his low values in the SH.

Curran *et al.* (1979) created a simple albedo model for use in converting satellite radiance measurements to cloud amount. They used preliminary satellite data for ice and snow amount, assumed a land albedo of 0.18 and an ice and snow albedo of 0.75, included zenith angle effects on ocean albedo and did not radiation weight their average. The lack of radia-

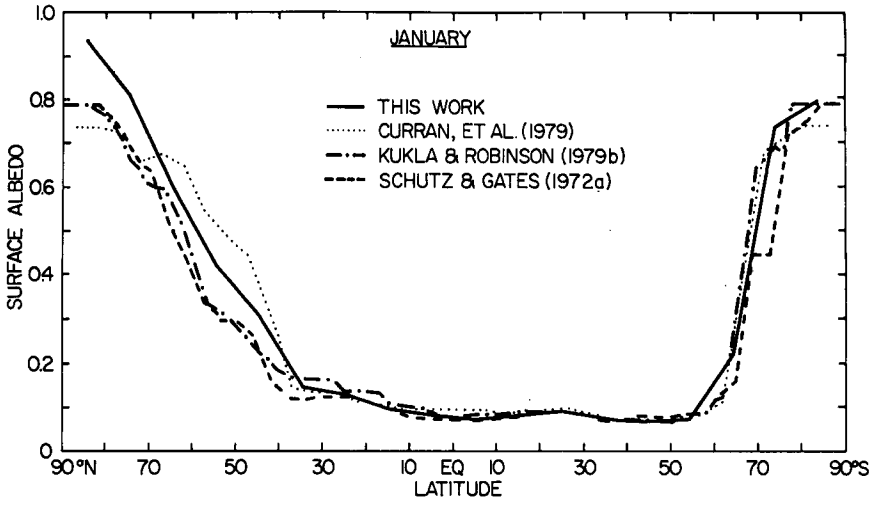

FIG. 15. Zonal average surface albedo for January compared to other calculations.

tion weighting and meltwater effect (discussed later, and see Fig. 20), and their high value for land albedo explains the differences with the current results. Curran *et al.* (1979) used their surface albedo model to calculate fractional cloud cover from satellite data. They neglected the meltwater effect on albedo in the summer, however, resulting in abnormally low cloud cover for the Arctic in the summer. If they would use the model developed here, this problem could be corrected.

The Hummel and Reck (1979) results include a detailed classification of land surfaces according to type and albedo for four quarters of the year and include meltwater effects. Their snow data are from ground observations and they did not radiation weight their results except to "include the fact that portions of the polar regions are not illuminated during their respective fall and winter." This explains why their NH polar albedos are lower than the current unweighted values.

Kukla and Robinson (1979b) used satellite data to give snow and ice amounts during a one year period during 1974–75. They did not include meltwater effects and did not radiation weight their average. Their results closely correspond to the current unweighted results. Their lack of a meltwater affect in the summer is balanced by an abnormally high winter albedo in the current results caused by the zenith angle correction to snow and ice albedo. These values do not contribute to the radiation-weighted average but make the unweighted average unreasonably high (see Fig. 21, Table 9).

Posey and Clapp (1964) presented surface albedo values for four months based on land categories taken from ground observations. Schutz and Gates calculated zonal averages from their maps for

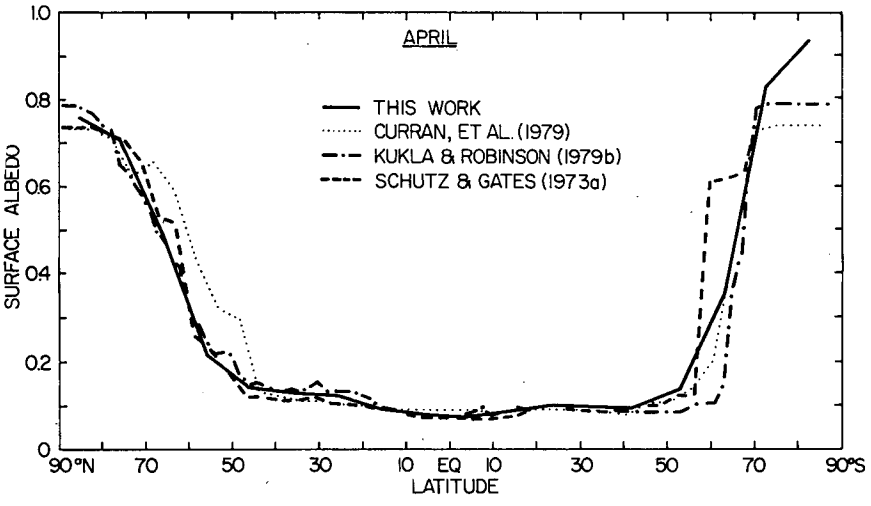

FIG. 16. As in Fig. 15 except for April.

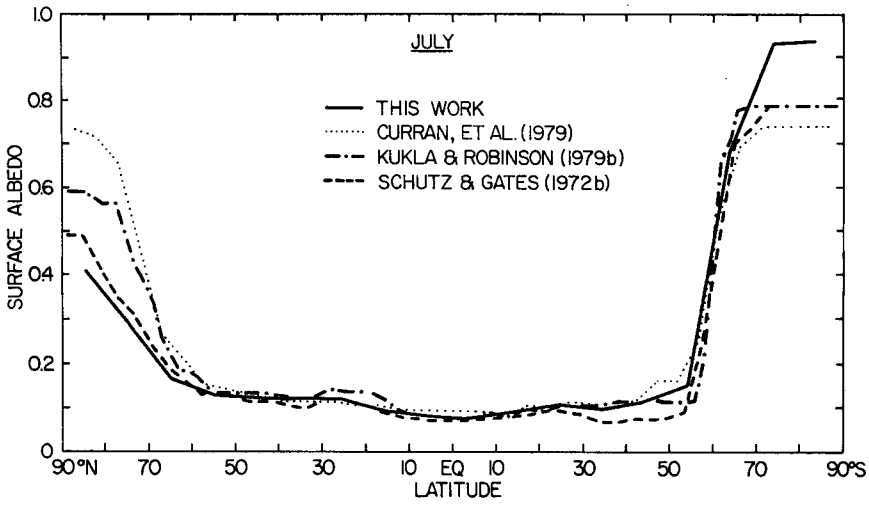

FIG. 17. As in Fig. 15 except for July.

January (1972a), April (1973a), July (1972b) and October (1974a). An annual average was calculated from these without weighting by radiation and is also included in Fig. 19. It closely corresponds to the current unweighted results except at the poles where the zenith angle correction caused high values. Posey and Clapp did include meltwater effects on their ice albedos.

Fig. 20 illustrates the effects on the radiation weighted annual averages of various assumptions used in calculating the snow and ice albedos. Both the zenith angle correction for snow and ice albedo and the cloud correction for snow and ice albedo had small effects, and the combined effects (both in the same direction) made very little difference in the annual average albedo. Therefore, I conclude that it is not important to include these effects when calculating albedo for studying global climate. For smaller time and space scales, however, these effects can be very important. The meltwater corrections, on the other hand, have a large effect in reducing the albedos. The ice meltwater is the dominant correction at 85°N, 75°N, 65°S and 75°S while the snow meltwater correction is dominant at 65–35°N. Fig. 21 illustrates these effects for the annual average unweighted by radiation. Here the zenith angle correction for snow and ice albedo appears quite large, but this is misleading since most of the high albedos occur during darkness. The cloud correction is seen to be small again as it does not change much with the seasons. The meltwater corrections appear misleadingly small because they occur during the summer.

A comparison of the globally averaged albedo calculated in this paper, with various assumptions and in other papers appears in Table 9. The impor-

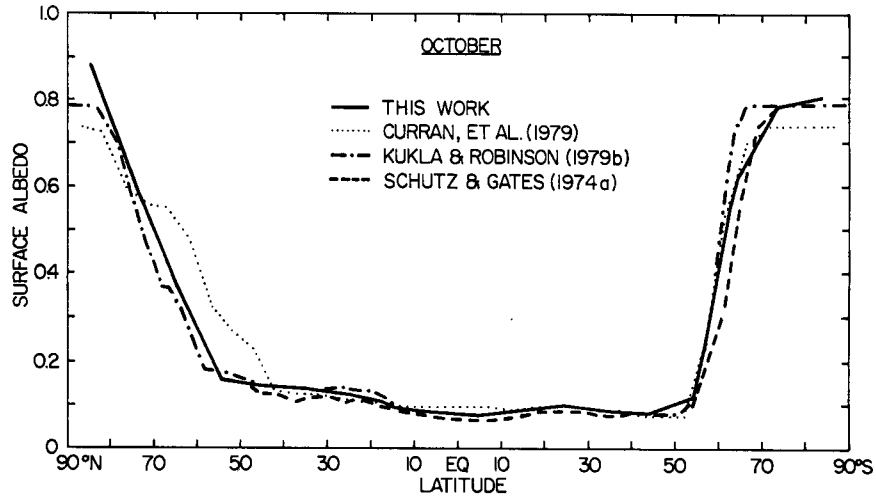

FIG. 18. As in Fig. 15 except for October.

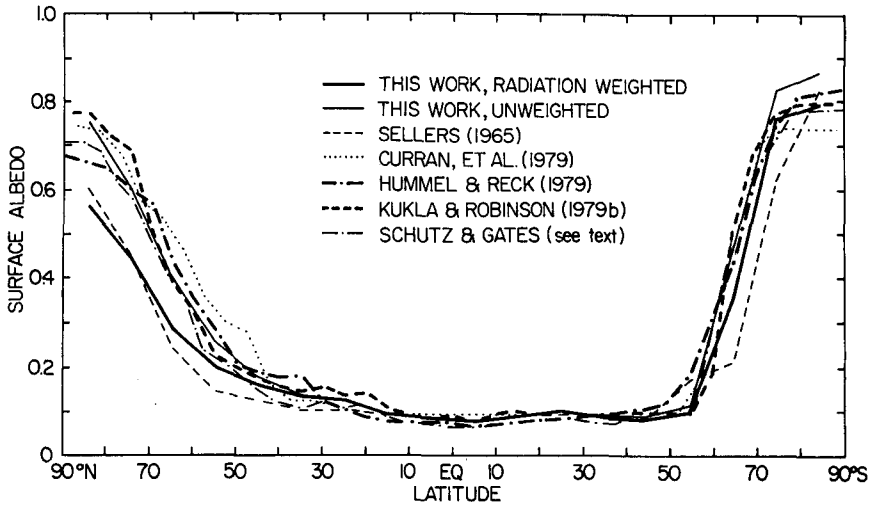

FIG. 19. Annual average surface albedo, radiation weighted, compared to unweighted average and other calculations.

tance of including radiation weighting is illustrated as well as the differences described earlier in this section. A globally averaged surface albedo of 0.150 seems to be the most reasonable value taking into account all the important effects.

7. The relationship between seasonal snow and ice cover and surface temperature

The previously presented results allow the calculation of zonally averaged surface albedo for any land or ocean 10° latitude band for any month given the surface temperatures and the ice and snow fractional areas. As a first step in developing a complete surface albedo parameterization for use in an energy balance climate model, the following analysis presents linear regressions of the zonally averaged snow cover with zonally averaged land surface air temperature, and of the zonally averaged sea ice cover with zonally averaged ocean surface air temperature. The relationships are complex and in a test of the NH relationships appear quite different between NH and SH for the case of sea ice. (SH snow data are not available.) Due to the questionable quality of the ESMR results for SH ice, the question of whether it is possible to parameterize snow and ice areas as a function of surface temperature alone is left for future consideration.

A linear regression was performed at each latitude relating snow cover to land air temperature and ice cover to ocean air temperature during the seasonal cycle. Those months and latitudes with complete or no ice or snow cover were excluded, and are shown

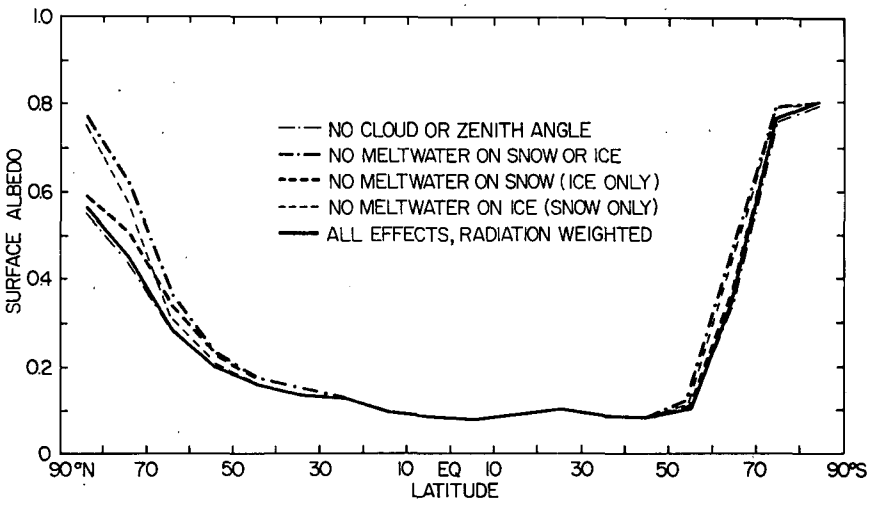

FIG. 20. Radiation weighted annual average surface albedo for different assumptions used in the calculations.

TABLE 9. Global average albedos calculated in this work with (4) using various assumptions compared with those from other works. The value for Hummel and Reck (1979) was only partially radiation weighted and so is indicated between the two columns. The Schutz and Gates values were averaged from values for four months and are based on data from Posey and Clapp (1964). The individual Schutz and Gates references are given in the text.

	Global albedo	
	Radiation weighted	Un-weighted
This work—all effects	0.1501	0.1709
This work—no cloud correction to snow and ice albedo	0.1491	0.1700
This work—no zenith angle correction to snow and ice albedo	0.1497	0.1662
This work—no cloud or zenith angle correction	0.1487	0.1652
This work—no meltwater correction for snow albedo	0.1575	0.1768
This work—no meltwater correction for ice albedo	0.1594	0.1762
This work—no meltwater correction for snow or ice albedo	0.1667	0.1821
Sellers (1965)	0.13	
Schutz and Gates (see caption)		0.155
Curran *et al.* (1979)		0.184
Hummel and Reck (1979)	0.1540	
Kukla and Robinson (1979)		0.170

as the boxed regions in Tables 2, 3 and 4. The regressions were performed for lags from −6 months through +5 months. The highest reduction of variance (R) was found for snow to be at either 0 or +1 (temperature leading snow) with all the other lags giving much poorer results. For NH oceans, the highest R was found at lag +1 (which is really a 1.5-month lag with temperature leading ice, because the ice data are for the end rather than the middle of the month) with all other lags giving much poorer results, and for SH oceans the highest R was for lag 1 with lag 2 slightly lower and all other lags much lower.

The resulting regression coefficients (A,B) for each latitude, given by

$$F_s = A + BT_L, \tag{6}$$

$$F_i = A + BT_s, \tag{7}$$

where F_s is the fractional snow area, F_i the fractional ice area and T_L and T_s are in °C, are shown as functions of the annual average temperature in Figs. 22, 23 and 24, which also give the reduction of variance for each relationship. A strong relationship at each latitude between temperature and ice and snow cover appears as expected, as shown by the large reductions of variance. The regression coefficients exhibit a strong functional dependence on annual average temperature. The A coefficients for both snow and ice decrease with higher annual mean temperatures, as expected. The B coefficients, which are the measure of the sensitivity of the snow and ice cover to seasonally changing temperature, behave differently for ice and snow. For snow, B is generally higher in magnitude than for ice in the NH showing the effects of a much larger seasonal cycle of snow cover. Because the land temperature exhibits a larger seasonal cycle than the ocean temperature, the snow cover would show a larger seasonal cycle with the same B as for the ice. The larger magnitude of B shows that the snow has a much larger cycle and stronger dependence on temperature. In addition, for snow B decreases in magnitude with increasing annual mean temperature, showing that the snow-albedo feedback becomes less important in the regions where solar radiation is the highest. B for the

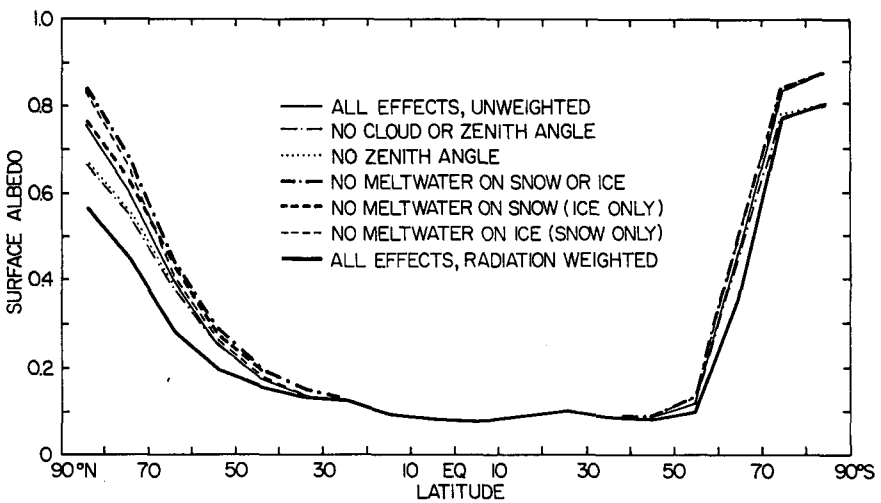

FIG. 21. Annual average surface albedo not weighted by radiation for different assumptions used in the calculations.

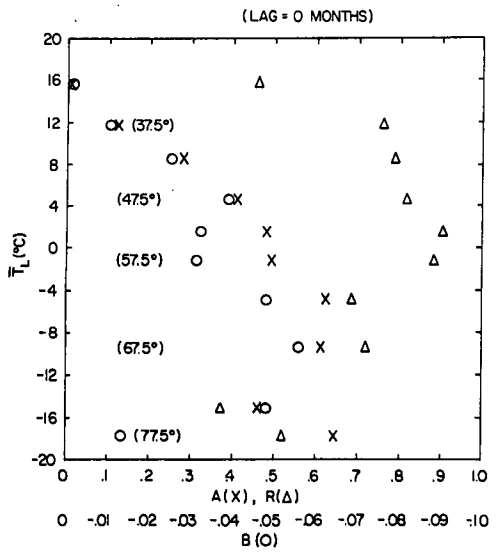

FIG. 22. Regression coefficients (A,B) and reduction of variance (R) for Northern Hemisphere snow cover and land temperature from (6) plotted against annual mean land temperature ($\bar{T}_L$). Also plotted are the latitude bands of the regressions.

ice, on the other hand increases in magnitude with increasing annual mean temperature, thus increasing the importance of correctly identifying the ice sheet edge in order to calculate the ice-albedo feedback properly. Overall, however, not only must the values of the regression coefficients and their latitudinal distributions be considered, but also the relative areas of snow and ice at each latitude, their albedos, and the contrast with the underlying surface must also be included in evaluating their relative contributions to the strength of the albedo feedback.

One might be tempted to parameterize the ice and snow areas by making A and B functions of annual mean temperature and using the linear relationships (6) and (7) at each latitude. If the functions were derived from the NH data, however, (7) would not accurately reproduce the SH sea ice (cf. Fig. 23 and Fig. 24). This indicates that factors other than surface temperature are important in determining fractional coverage of sea ice, and must be considered in a parameterization. While A and B change in the same sense in Figs. 23 and 24 as a function of annual mean temperature, and B and R are both highest at latitudes 60–65° in both hemispheres, B is about three times larger for the SH than for the NH. This is partially due to the larger seasonal cycle of sea ice at these latitudes in the SH, but is even more due to the smaller SH temperature cycle. Although the SH ice data are preliminary and subject to reinterpretation of the relationship between ESMR radiance and sea ice cover, I do not think that better data will change the above results very much.

8. Annual average snow and ice cover and surface temperature

Many recent energy balance climate modeling studies make the annual average assumption used in the original models of this type by Sellers (1969) and Budyko (1969). For use in these models a linear regression analysis of annual average snow and ice cover with surface temperatures follows.

Table 10 presents the annual zonal average snow cover, ice cover, snow and ice zonal average weighted by area, and land, ocean and zonal average temperatures. NH snow cover data are used in the SH, but

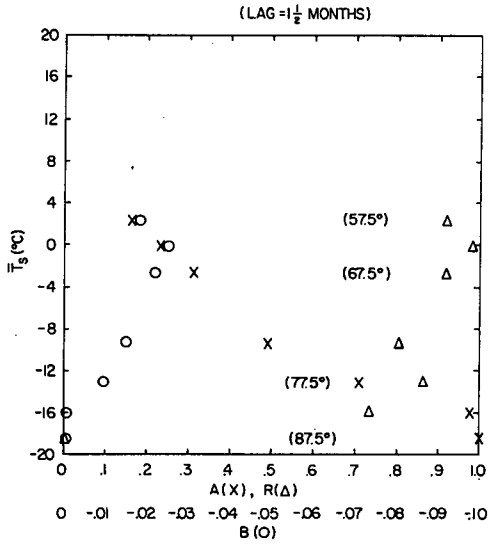

FIG. 23. Regression coefficients (A,B) and reduction of variance (R) for the Northern Hemisphere ice cover and sea temperature from (7) plotted against annual mean sea temperature ($\bar{T}_S$).

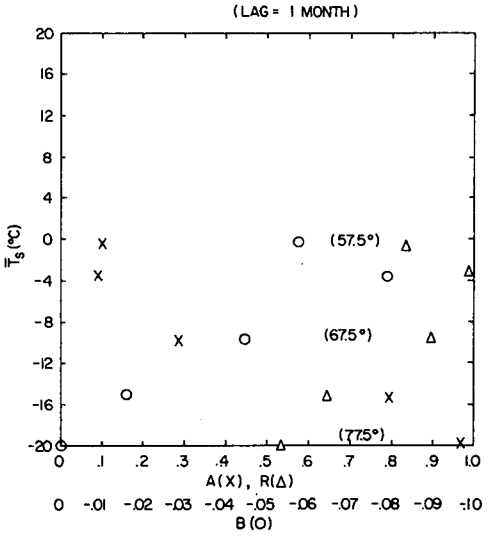

FIG. 24. As in Fig. 23 except for the Southern Hemisphere.

there is little land in these SH latitudes as indicated by the combined zonal average ice and snow covers which favors the ice cover except for Antarctica. The temperature data sources are described in Section 5, and the snow and ice data come from Tables 2, 3 and 4.

Table 11 presents annual average linear regressions of snow and ice cover with temperature of the same form as (6) and (7). Various latitude ranges were used for the zonal average calculations as the snow and ice coverage was very low in the lower latitudes. Antarctica was excluded from 80–90°S as its permanent snow cover is unrelated to temperature. The permanent snow features in the NH were eliminated by using Table 2 and not Table 1. A SH snow with $\bar{T}_L$ regression was not attempted due to the SH snow data used and the small SH snow area.

TABLE 10. Annual average zonal average snow cover, ice cover, combined snow and ice weighted by areas of land and ocean, and land, ocean and zonal average temperatures. The SH snow is a reflection of NH snow. The snow and ice data come from Tables 2, 3 and 4 and the temperature data are described in Section 5.

Latitude	Snow cover	Ice cover	Snow and ice	Temperature (°C) Land ($\bar{T}_L$)	Ocean ($\bar{T}_s$)	Zonal average ($\bar{T}_z$)
87.5°N	1.000	1.000	1.000	−21.71	−18.63	−18.63
82.5°N	1.000	0.991	0.991	−19.49	−16.44	−16.89
77.5°N	0.875	0.839	0.841	−17.85	−13.18	−14.25
72.5°N	0.804	0.631	0.680	−15.19	−9.28	−11.32
67.5°N	0.730	0.394	0.628	−9.44	−3.40	−7.70
62.5°N	0.644	0.227	0.512	−4.84	0.20	−3.27
57.5°N	0.532	0.116	0.345	−1.17	2.72	0.58
52.5°N	0.427	0.0	0.254	1.74	5.93	3.45
47.5°N	0.297	0.0	0.167	4.81	8.75	6.54
42.5°N	0.131	0.0	0.064	8.73	12.32	10.57
37.5°N	0.037	0.0	0.016	12.01	16.09	14.33
32.5°N	0.006	0.0	0.002	15.98	19.19	17.83
27.5°N	0.0	0.0	0.0	20.86	21.94	21.50
22.5°N	0.0	0.0	0.0	24.21	24.14	24.17
17.5°N	0.0	0.0	0.0	25.91	25.59	25.68
12.5°N	0.0	0.0	0.0	26.36	26.45	26.43
7.5°N	0.0	0.0	0.0	25.46	26.80	26.47
2.5°N	0.0	0.0	0.0	24.67	26.72	26.28
2.5°S	0.0	0.0	0.0	24.75	26.68	26.22
7.5°S	0.0	0.0	0.0	24.26	26.44	25.94
12.5°S	0.0	0.0	0.0	23.19	25.64	25.14
17.5°S	0.0	0.0	0.0	22.61	24.40	23.98
22.5°S	0.0	0.0	0.0	21.30	22.74	22.38
27.5°S	0.0	0.0	0.0	19.17	20.67	20.35
32.5°S	0.006	0.0	0.001	16.85	18.11	17.91
37.5°S	0.037	0.0	0.002	14.25	15.04	14.98
42.5°S	0.131	0.0	0.005	11.47	11.54	11.54
47.5°S	0.297	0.0	0.007	8.78	7.88	7.90
52.5°S	0.427	0.0	0.006	6.24	4.44	4.47
57.5°S	0.532	0.080	0.080	0.92	0.97	0.97
62.5°S	0.644	0.370	0.371	−6.89	−3.42	−3.43
67.5°S	0.730	0.722	0.724	−20.11	−9.81	−11.92
72.5°S	0.804	0.965	0.866	−32.44	−14.68	−25.59
77.5°S	0.875	0.992	0.888	−39.10	−20.08	−37.07
82.5°S	1.000	1.000	1.000	−42.30		−42.30
87.5°S	1.000	1.000	1.000	−46.38		−46.38

TABLE 11. Results of linear regressions of annual average snow and ice with temperatures. R is the reduction of variance of the regression $F = A + BT$, where F is the fractional snow or ice and T is temperature. $\bar{T}_L$, $\bar{T}_s$ and $\bar{T}_z$ are respectively the annual mean land, ocean and zonally averaged surface temperatures.

Annual average regression of	Latitude range	A	B	R
NH snow and $\bar{T}_L$	30°N–80°N	0.434	−0.0278	0.971
NH ice and $\bar{T}_s$	55°N–90°N	0.240	−0.0434	0.994
NH zonal snow and ice and $\bar{T}_z$	40°N–90°N	0.381	−0.0327	0.990
	35°N–90°N	0.395	−0.0313	0.986
	30°N–90°N	0.412	−0.0294	0.976
SH ice and $\bar{T}_s$	55°S–80°S	0.200	−0.0453	0.942
SH ice and $\bar{T}_z$	55°S–80°S	0.269	−0.0231	0.858
SH zonal snow and ice and $\bar{T}_z$	30°S–80°S	0.254	−0.0202	0.889
	35°S–80°S	0.238	−0.0212	0.893
	40°S–80°S	0.222	−0.0221	0.890
	45°S–80°S	0.212	−0.0225	0.875
	50°S–80°S	0.221	−0.0221	0.844
	55°S–80°S	0.280	−0.0198	0.799

All the regressions show a strong relationship with the NH calculations having higher reductions of variance. NH ice with $\bar{T}_s$ and SH ice with $\bar{T}_s$ show very similar results indicating that while the seasonal ice $-T_s$ relationships are different in each hemisphere, the annual average relationships are the same. Therefore, an annual average model which distinguishes between land and water temperatures could use these regression relationships to parameterize snow and ice cover. The zonal average regressions show interhemispheric differences. Because the SH polar temperature gradient is so much larger the sensitivity (B) of the averaged snow and ice cover to temperature is lower. This indicates that a purely zonal average model may be too simple to adequately reproduce a major feature of the climate system.

9. Summary and discussion

The seasonal cycle of mean Northern Hemisphere snow cover based on satellite data has been presented both as maps and as zonal averages. These data have applications for both energy balance and general circulation climate modeling. The snow cover is an important determinant of the planetary albedo of the climate system, as even the albedo of cloudy regions depends to a large extent on surface albedo. It is suggested, however, that due to an equatorward decrease of snow cover dependence on temperature coupled with a decreased snow albedo due to forests and meltwater on the snow, that the climate is not as sensitive to the location of the snow boundary as to that of sea ice. This will be tested in the future with modeling studies.

Zonal average sea ice cover for the Northern Hemisphere based on extensive surface as well as satellite observations have also been presented. The importance of these data to climate studies is similar to the snow data as discussed above. The sea ice, however, is found to be very sensitive to temperature along the ice-water boundary, and the correct determination of the value of parameters to be used in a parameterization of ice cover as function of temperature is crucial to the accurate simulation of the ice-albedo feedback. Unfortunately, a search for a corroborating relationship in the Southern Hemisphere reveals the same functional relationship but very different numerical values of the parameters. This leads to the conclusion that it may not be possible to model the seasonal cycle of sea ice cover as a function of temperature only and that other factors must be considered. A philosophical question in energy balance climate modeling thus presents itself: Does one use different relationships in each hemisphere based on the data analysis in the interest of simplicity or does one search for a more complicated relationship which works for both hemispheres? Obviously the second approach will in the long run best benefit scientific knowledge, but this dilemma illustrates the limitations of attempting to use simple models (energy balance climate models in which everything is parameterized in terms of surface temperature) to model complex systems.

Data are presented on the distribution of land surface types and their albedos that allow a calculation of the surface albedo of any land or water 10° latitude band for any month given the surface air temperature (to calculate the meltwater effect) and the ice and snow cover. The surface type data, while quite detailed, are based on the current climate and human land use. Studies of climates quite different from the present will have to account for changes in these land use patterns. The albedos used for the various land types, while based on the best available data, do not include several potentially important effects. While the contrast between snow and snow-free albedos is believed to be much larger than the errors in the land albedos, much work still remains to be done in measuring representative albedos of different surface types under different conditions.

Inclusion of the meltwater effect and weighting by solar radiation are emphasized as crucial to calculate accurately the zonally averaged annual average surface albedo. It is also important to use lower values for snow albedo when the snow is in forests than when it is on flat terrain. The present calculations are the most comprehensive set yet, including the above effects and using detailed new observations of snow and ice cover. The particular values chosen for snow and ice albedos may be open to question, but were based on the best available data. The use of corrected values awaits future more detailed observational studies.

Acknowledgments. This research was made much easier because of the assistance of several people. I would like to thank Mike Matson for providing me with unpublished snow cover maps, John Hummel for digitized data on land surface types, Bob Curran for a preprint containing SH sea ice data, John Walsh and Claudia Johnson for calculating NH zonal averages of sea ice cover for me, Don Petzold for valuable discussions of zenith angle effects on snow albedo, Starley Thompson for surface temperature data, and George Kukla for valuable discussions of SH sea ice data. I thank Alan Krol for assistance in calculations and drawing some of the figures, Claire Villanti for drafting the figures, and Earlene Bradley and Merida Gonzalez for typing the manuscript. This research was supported by NASA Grant NSG-5209.

REFERENCES

British Meteorological Office, 1977: *Monthly Ice Charts*. HMSO, London.

Budyko, M. I., 1969: The effect of solar radiation variations on the climate of the earth. *Tellus*, **21**, 611–619.

Cess, R. D., 1978: Biosphere-albedo feedback and climate modeling. *J. Atmos. Sci.*, **35**, 1765–1768.

Chernigovskii, N. T., 1963: Radiational properties of the central Arctic ice coat. *Tr. Ark. Antark. Nauchno-Issled. Inst.*, **253**, 249–260.

CLIMAP Project Members, 1976: The surface of the ice-age earth. *Science*, **191**, 1131–1137.

Cohen, S. B., Ed., 1973: *Oxford World Atlas*. Oxford University Press, 190 pp.

Crutcher, H. L., and J. M. Meserve, 1970: *Selected-Level Heights, Temperatures and Dew Point Temperatures for the Northern Hemisphere*. NAVAIR 50-1C-52, Washington, DC. [Available from Chief, Naval Operations].

Curran, R. J., R. Wexler and M. L. Nack, 1979: Albedo climatology analysis and the determination of fractional cloud cover. NASA Tech. Memo. 79576. Submitted to *J. Appl. Meteor.*

Doronin, Y. P., 1970: *Thermal Interaction of the Atmosphere and the Hydrosphere in the Arctic*. Israeli Program for Scientific Translations, Jerusalem, 244 pp.

Hammond Contemporary World Atlas, 1972: Doubleday and Co., 256 pp.

Hummel, J. R., and R. A. Reck, 1979: A global surface albedo model. *J. Appl. Meteor.*, **36**, 239–253.

Kondrat'yev, K. Y., 1965: *Actionmetry*. NASA TT F-9712, Washington, D.C., 675 pp. [NTIS N66-10158].

Kukla, G. J., and H. J. Kukla, 1974: Increased surface albedos in the Northern Hemisphere. *Science*, **183**, 709–714.

——, and D. Robinson. 1979a: Accuracy of snow and ice monitoring. *Glaciological Data*, Rep. DG-5, 91–97.

——, and ——, 1979b: Annual cycle of surface albedo. Submitted to *Mon. Wea. Rev.*

Kung, E. C., R. A. Bryson and D. H. Lenschow, 1964: Study of a continental surface albedo on the basis of flight measurements and structure of the earth's surface cover over North America. *Mon. Wea. Rev.*, **92**, 543–564.

Lian, M. S., and R. D. Cess, 1977: Energy balance climate models: a reappraisal of ice-albedo feedback. *J. Atmos. Sci.*, **34**, 1058–1062.

London, J. L., 1957: A study of the atmospheric heat balance. Final Report, Contract AF 19(122)-165, College of Engineering, New York University.

Matson, M., 1977: Winter snow-cover maps of North America and Eurasia from satellite records, 1966–1976. NOAA Tech. Memo. NESS 84, Washington, DC, 28 pp.

Miranova, Z. F., 1973: Albedo of earth's surface and clouds. Chapter 4, *Radiation Characteristics of the Atmosphere and the Earth's Surface*, Kondat'ev K. Ya., Ed., Amerind Publ., Co., New Delhi, 580 pp.

Payne, R. E., 1972: Albedo of the sea surface. *J. Atmos. Sci.*, **29**, 959–970.

Petzold, D. E., 1977: An estimation techique for snow surface albedo. *Climatolog. Bull.*, **21**, 1–11.

Posey, J. W., and P. F. Clapp, 1964: Global distribution of normal surface albedo. *Geofis. Int.*, **4**, 33–48.

Rusin, N. P., 1964: *Meteorological and Radiational Regime of Antarctica*. Israeli Program for Scientific Translations, Jerusalem, 355 pp.

Sasamouri, T., J. London and D. V. Hoyt, 1972: Radiation budget of the Southern Hemisphere. *Meteor. Monogr.*, No. 35, 9–23.

Schneider, S. H., and R. R. Dickinson, 1974: Climate modeling. *Rev. Geophys. Space Phys.*, **12**, 447–493.

Schutz, C., and W. L. Gates, 1971: Global climatic data for surface, 800 mb, 400 mb: January. R-915-ARPA, The Rand Corporation, Santa Monica, CA, 173 pp.*

——, and ——, 1972a: Supplemental global climatic data: January. R-915/1-ARPA, The Rand Corporation, Santa Monica, CA, 41 pp.*

——, and ——, 1972b: Global climatic data for surface, 800 mb, 400 mb: July. R-1029-ARPA, The Rand Corporation, Santa Monica, CA, 180 pp.*

——, and ——, 1973a: Global climatic data for surface, 800 mb, 400 mb: April, R-1317-ARPA, The Rand Corporation, Santa Monica, CA, 192 pp.*

——, and ——, 1973b: Supplemental global climatic data: January. R-915/2-ARPA, The Rand Corporation, Santa Monica, CA 38 pp.*

——, and ——, 1974a: Global climatic data for surface, 800 mb, 400 mb: October. R-1425-ARPA, The Rand Corporation, Santa Monica, CA, 192 pp.*

——, and ——, 1974b: Supplemental global climatic data: July. R-1029/1-ARPA, The Rand Corporation, Santa Monica, CA, 38 pp.*

Sellers, W. D., 1965: *Physical Climatology*, University of Chicago Press, 272 pp.

——, 1969: A global climatic model based on the energy balance of the earth-atmosphere system. *J. Appl. Meteor.*, **8**, 392–400.

Taljaard, J. J., H. van Loon, H. L. Crutcher and R. L. Jenne, 1969: *Climate of the Upper Air: Southern Hemisphere, Vol. I, Temperatures, Dew Points, and Heights at Selected Pressure Levels*. NAVAIR 50-1C-55, Washington, D.C. [Available from Chief, Naval Operations].

Vowinckel, E., and S. Orvig, 1970: The climate of the North Polar Basin. *World Survey of Climatology*, Vol. 14, H. Landsberg, Ed., Elsevier, 129–252.

Walsh, J. E., 1978: A data set on Northern Hemisphere sea ice extent, 1953–76. *Glaciological Data*, Rep. GD-2, 49–51.

——, and C. M. Johnson, 1979: An analysis of Arctic sea ice fluctuations, 1953–77. *J. Phys. Oceanogr.*, **9**, 580–591.

Weisnet, D. R., and M. Matson, 1976: A possible forecasting technique for winter snow cover in the Northern Hemisphere and Eurasia. *Mon. Wea. Rev.*, **104**, 828–835.

Williams, J., R. G. Barry and W. M. Washington, 1974: Simulation of the atmospheric circulation using the NCAR global circulation model with ice age boundary conditions. *J. Appl. Meteor.*, **13**, 305–317.

* Available from The Rand Corporation, 1700 Main Street, Santa Monica, CA 90406.